Supporting Information for

Photosensitizing Ruthenium(II)-Dye Multilayers: Photoinduced Charge Separation and Back Electron Transfer Suppression

Nobutaka Yoshimura, Atsushi Kobayashi, Wataru Genno,‡ Takashi Okubo,‡ Masaki Yoshida, Masako Kato**

Department of Chemistry, Faculty of Science, Hokkaido University, North 10 West 8, Kita-ku, Sapporo, Hokkaido 060-0810, Japan

‡School of Science and Engineering, Kindai University, 3-4-1 Kowakae, Higashi-Osaka-shi, Osaka 577-8502, Japan.

Contents

Table S6. Amount of Ru(II) photosensitizer immobilized on TiO_2-ITO electrode.

Table S7. The photovoltaic data of DSSCs based on Ru(II)-PS-multilayered TiO_2-ITO photoelectrodes under AM1.5G irradiation.

Figure S12. IPCE action spectra of **RuCP^2**@TiO_2-ITO, **RuCP^2**-Zr-**RuP^6**@TiO_2-ITO, and **RuCP^2**-Zr-**RuP^4**-Zr-**RuP^6**@TiO_2-ITO as the photoanode in comparison with UV-Vis diffuse reflectance spectra of these photoelectrodes and absorption spectra of **RuP^6**, **RuP^4**, and **RuCP^2** in water.

Scheme S1. Schematic energy diagram showing plausible energy and electron transfers of **RuCP^2**-Zr-**RuP^6**@Pt-TiO_2.

Preparation of Ru(II)-PS-multilayered TiO_2-ITO photoelectrodes.

1. Preparation of TiO_2-ITO electrode: ITO electrodes (sheet resistance = 10 Ω cm^{-1}) were washed under ultrasound irradiation with acetone, pure water, KG aq, LC-2 aq, ultra-pure water, and isopropyl alcohol (IPA). Then electrodes were dried in 90 °C and further cleaned by UV light irradiation (PL16-110, AsOne) for 15 min. TiO_2 paste (PECC-C01-06, Peccell Technologies) were pasted on the cleaned ITO electrodes, dried in R.T. for 15 min, and then sintered at 150 °C for 10 min to obtain TiO_2-ITO electrodes.[1]

2a. Fabrication of **RuCP^2**@TiO_2-ITO: A TiO_2-ITO electrode was immersed in the aqueous solution containing 0.2 mM Ru(II) PS (**RuCP^2**) and 0.1 M $HClO_4$ for overnight at 293 K and followed by rinsing with pure water and then dried at 100 °C.

2b. Fabrications of **RuCP^2**-Zr-**RuP^6**@TiO_2-ITO and **RuCP^2**-Zr-**RuP^4**-Zr-**RuP^6**@TiO_2-ITO electrodes: These Ru(II)PS-multilayered electrodes were prepared by alternating immersion of a TiO_2-ITO electrode to Ru(II)PS aqueous solution (0.2 mM Ru(II) PS in 0.1 M $HClO_4$ aq. for overnight) and 5 mM $ZrCl_2O$ MeOH solution (for 60 min) at 293 K. **RuP^6, RuP^4** and **RuCP^2** were used for the 1st, 2nd and 3rd PS layers, respectively, for **RuCP^2**-Zr-**RuP^4**-Zr-**RuP^6**@TiO_2-ITO electrodes. **RuP^6** and **RuCP^2** were used for the 1st and 2nd PS layers for **RuCP^2**-Zr-**RuP^6**@TiO_2-ITO electrodes. Obtained electrodes were washed with MeOH and dried at 100 °C after immersion.

4. Dye-sensitized solar cell fabrication: For preparation of the counter electrode, an aqueous solution of poly(3,4-ethylenedioxythiophene)tetramethacrylate (PEDOT-TMA, Aldrich 649821) was mixed with ethanol in a volume ratio of 4:1. The mixture was spin-coated (3000 rpm for 10 s) on ITO glass and annealed at 50°C for 10 min. This spin-coating process was repeated for three times. The Ru(II)-dye-multilayered TiO_2-ITO and PEDOT-TMA electrodes were assembled to fabricate a sandwich-type cell with a 50 μm spacer. The electrolyte consisted of a solution of lithium iodide (LiI, 0.5 M), iodine (I_2, 0.05 M) and 0.5 M *t*-butyl pyridine in methoxy-acetonitrile or lithium iodide (LiI, 0.5 M), and iodine (I_2, 0.05 M) in water, and it was injected between the electrodes.

Calculation of the amount of Ru(II) complex immobilized on the Pt-TiO_2 nanoparticles

To estimate the amount of immobilized Ru(II) complexes on Pt-TiO_2 nanoparticle, UV-Vis absorption spectra of each supernatant solution used for the immobilization reaction was measured (see Figure S1 shown below). The Ru(II) complex concentration used for the UV-Vis absorption spectral measurement (C_A) is estimated by Equation (1) based on the Lambert-Beer law.

$$A = C_A \cdot l \cdot \varepsilon \quad (Eq.\ 1)$$

A = absorbance, C_A = concentration of the Ru(II) complex,

l = cell path length (1 cm), ε = molar absorption coefficient

The absorbance at the ^{1}MLCT absorption band of each complex (**RuCP^2**: 456 nm, **RuP^4**: 462 nm, **RuP^6**: 463 nm,) and their corresponding molar absorption coefficients (**RuCP^2**: 14,600; **RuP^4**: 15,900; **RuP^6**: 19,600) enable us to estimate the concentration of the Ru(II) complex that was not immobilized in the reaction. Since a 50-fold diluted aqueous solution was used in each measurement, the concentration of the original supernatant solution (C_B) is calculated by $C_B = C_A \times 50$. The total volume of the supernatant solution is 6.05 mL (see the Experimental section). Thus, the amount of Ru(II) complexes in the supernatant solution (M_S) is estimated by Equation (2).

$$M_s = C_B \times \frac{6.05}{1000}\ (\mathrm{mol}) \quad (Eq.\ 2)$$

Finally, the molar amount of the Ru(II) complex immobilized on the TiO_2 surface (M_i) can be estimated by Equation (3).

$$M_i = M_o - M_s\ (\mathrm{mol}) \quad (Eq.\ 3)$$

where M_o denotes the molar amount of the Ru(II) complex in the 1.25 mM Ru(II) aqueous solution used for the immobilization reaction. The results are summarized in Table S1.

Table S1. Absorbance of each supernatant solution and the calculated C_B and M_i values.

	RuCP^2@Pt-TiO_2	**RuCP^2**-Zr-**RuP^6**@Pt-TiO_2		**RuCP^2**-Zr-**RuP^4**-Zr-**RuP^6**@Pt-TiO_2		
	1st layer (**RuCP^2**)	2nd outer layer (**RuCP^2**)	1st inner layer (**RuP^6**)	3rd outer layer (**RuCP^2**)	2nd middle layer (**RuP^4**)	1st inner layer (**RuP^6**)
A	0.098	0.120	0.328	0.264	0.154	0.328
C_B (mM)	0.335	0.411	0.837	0.904	0.485	0.837
M_i (μmol)	5.47	5.01	2.44	2.03	4.57	2.44

Calculation of the surface coverage of Ru(II) complexes per unit area of TiO_2

Assuming that the TiO_2 nanoparticles are spherical, we simply calculated the surface area on the TiO_2 nanoparticle (S_m) using Equation (4). In these calculations, the effect of the loaded Pt co-catalyst was omitted.

$$S_m = 4 \cdot \pi \cdot \left(\frac{a}{2} \times 10^{-7}\right)^2 \text{ (cm}^2\text{ per one particle)} \quad (Eq.\ 4)$$

a = Averaged particle diameter of TiO_2 nanoparticle (15 nm)

Since the calculated surface area (S_m) based on Equation (4) corresponds to only one TiO_2 nanoparticle, it is necessary to determine the number of TiO_2 nanoparticles (P_t) contained in 30 mg to estimate the total surface area of TiO_2 (S_t) used in the immobilization reaction of the Ru(II) complexes. The total volume of 30 mg of TiO_2 nanoparticles (V_t) can be calculated using Equation (5) based on the density of TiO_2 (anatase TiO_2 = 3.90 g/cm^3).

$$V_t = \frac{30 \times 10^{-3}\ \text{(g)}}{3.90\ \text{(g/cm}^3\text{)}}\ \text{(cm}^3\text{)} \quad (Eq.\ 5)$$

The number of TiO_2 nanoparticles (P_t) in 30 mg is also estimated using Equations (6) and (7) based on the volume of one TiO_2 nanoparticle (V_m) and the total volume (V_t).

$$V_m = \frac{4}{3} \cdot \pi \cdot \left(\frac{a}{2} \times 10^{-7}\right)^3 \text{ (cm}^3\text{ per one particle)} \quad (Eq.\ 6)$$

$$P_t = \frac{V_t}{V_m} \quad (Eq.\ 7)$$

Then, the total surface area of 30 mg of TiO_2 (S_t) can be estimated by Equation (8).

$$S_t = S_m \times P_t\ \text{(cm}^2\text{)} \quad (Eq.\ 8)$$

The amount of immobilized Ru(II) complexes per unit area of TiO_2 (Surface coverage: N) is estimated by Equation (9) based on the amount of immobilized Ru(II) complex (M_i) and the total surface area of 30 mg of TiO_2 (S_t). The estimated N and M_i values are summarized in Table 1.

$$N = \frac{M_i}{S_t}\ \text{(mol/cm}^2\text{)} \quad (Eq.\ 9)$$

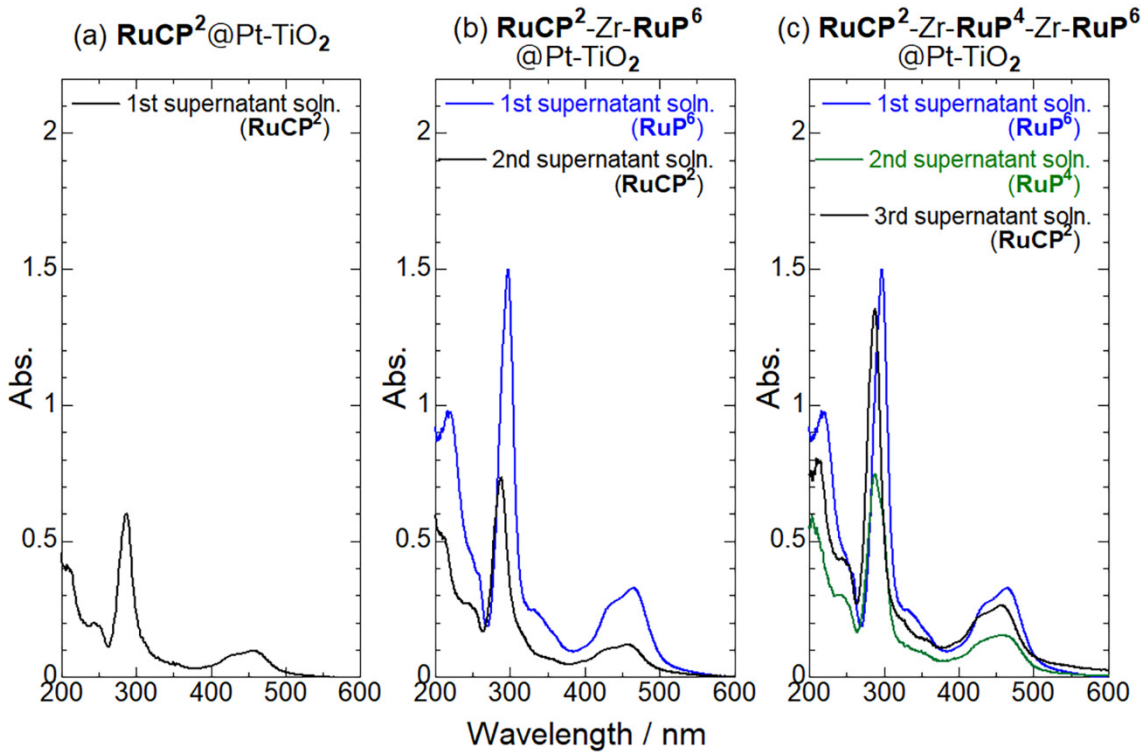

Figure S1. UV-Vis absorption spectra of the supernatant solutions at 298 K. (a) **RuCP²**@Pt-TiO_2, (b) **RuCP²**-Zr-**RuP⁶**@Pt-TiO_2, and (c) **RuCP²**-Zr-**RuP⁴**-Zr-**RuP⁶**@Pt-TiO_2. Note that each solution (1 mL) was diluted to 50 mL by the addition of deionized water before the spectral measurement.

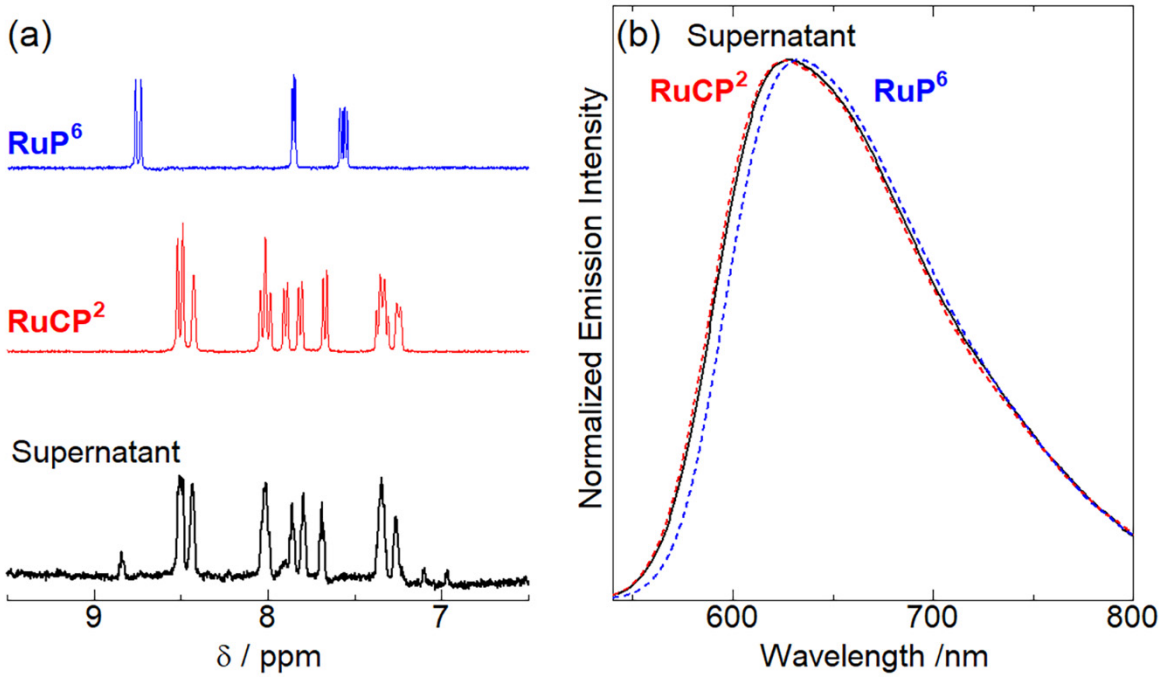

Figure S2. (a) ^{1}H NMR and (b) emission spectra of the supernatant solution (black lines) obtained from the immobilization reaction of **RuCP²** for the synthesis of **RuCP²**-Zr-**RuP⁶**@Pt-TiO_2 by ultracentrifugation. Blue and red lines are the spectra of **RuP⁶** and **RuCP²** in the aqueous solution.

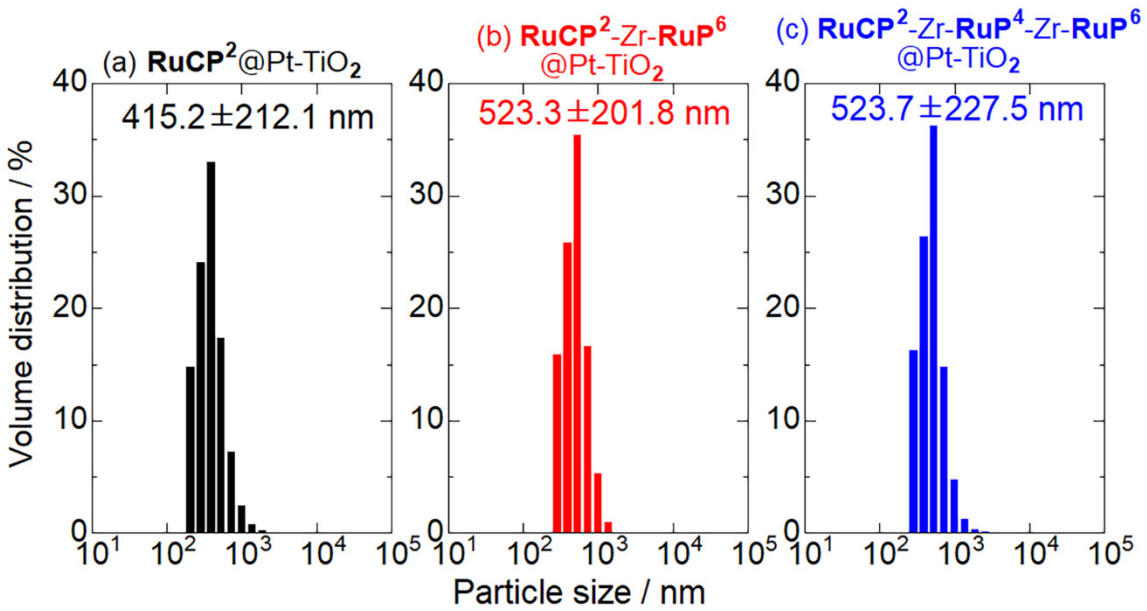

Figure S3. Particle diameter distributions estimated by the dynamic light scattering method for (a) **RuCP²**@Pt-TiO_2, (b) **RuCP²**-Zr-**RuP⁶**@Pt-TiO_2, and (c) **RuCP²**-Zr-**RuP⁴**-Zr-**RuP⁶**@Pt-TiO_2 nanoparticles in the diluted HCl aqueous solution (pH = 2).

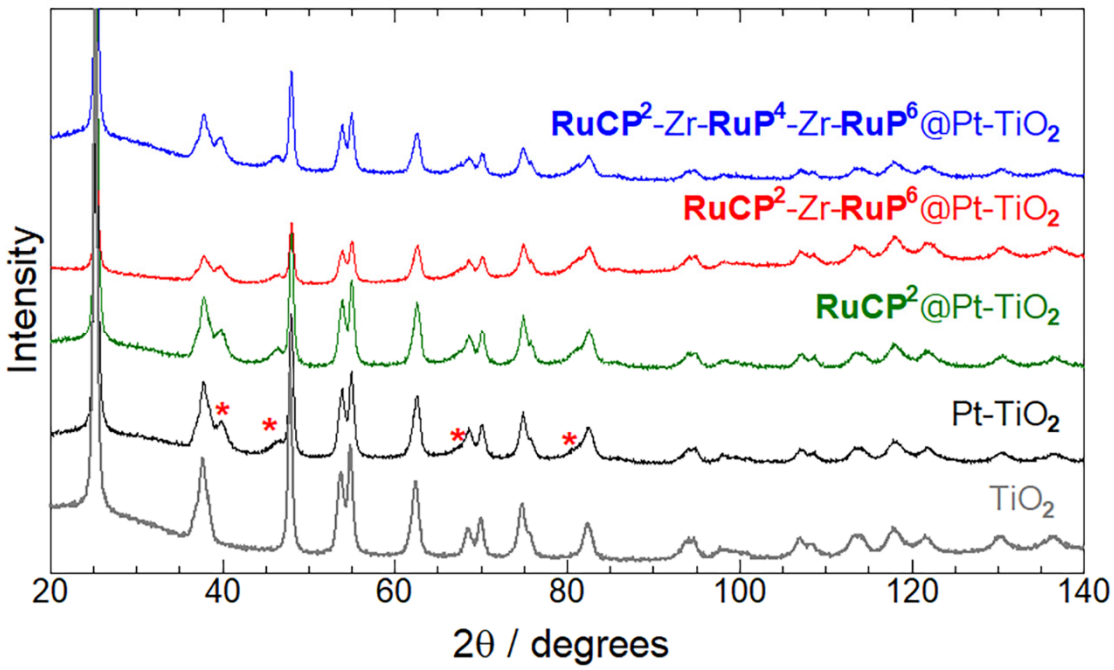

Figure S4. Experimental PXRD patterns of TiO_2, Pt-TiO_2, **RuCP²**@Pt-TiO_2, **RuCP²**-Zr-**RuP⁶**@Pt-TiO_2, and **RuCP²**-Zr-**RuP⁴**-Zr-**RuP⁶**@Pt-TiO_2 nanoparticles (Pt = 5wt%) in the solid state at 293 K. The red asterisks show the diffraction peaks derived from Pt cocatalyst loaded on the surface of TiO_2 nanoparticle.

Table S2. Estimated particle diameters of TiO_2 and Pt cocatalyst.

Photocatalyst	TiO_2 (nm)[a]	Pt (nm)[a]
TiO_2	21.3(1)	-
Pt-TiO_2	21.4(2)	6.0(7)
RuCP^2@Pt-TiO_2	21.8(1)	6.2(7)
RuCP^2-Zr-**RuP^6**@Pt-TiO_2	21.3(2)	6.5(6)
RuCP^2-Zr-**RuP^4**-Zr-**RuP^6**@Pt-TiO_2	21.7(2)	6.3(9)

[a] Diameters were estimated based on the diffraction peaks observed at 25.2° for TiO_2 and 46.2° for Pt cocatalyst (see Figure S4). The peak fitting was done by Pseudo Volgt function.

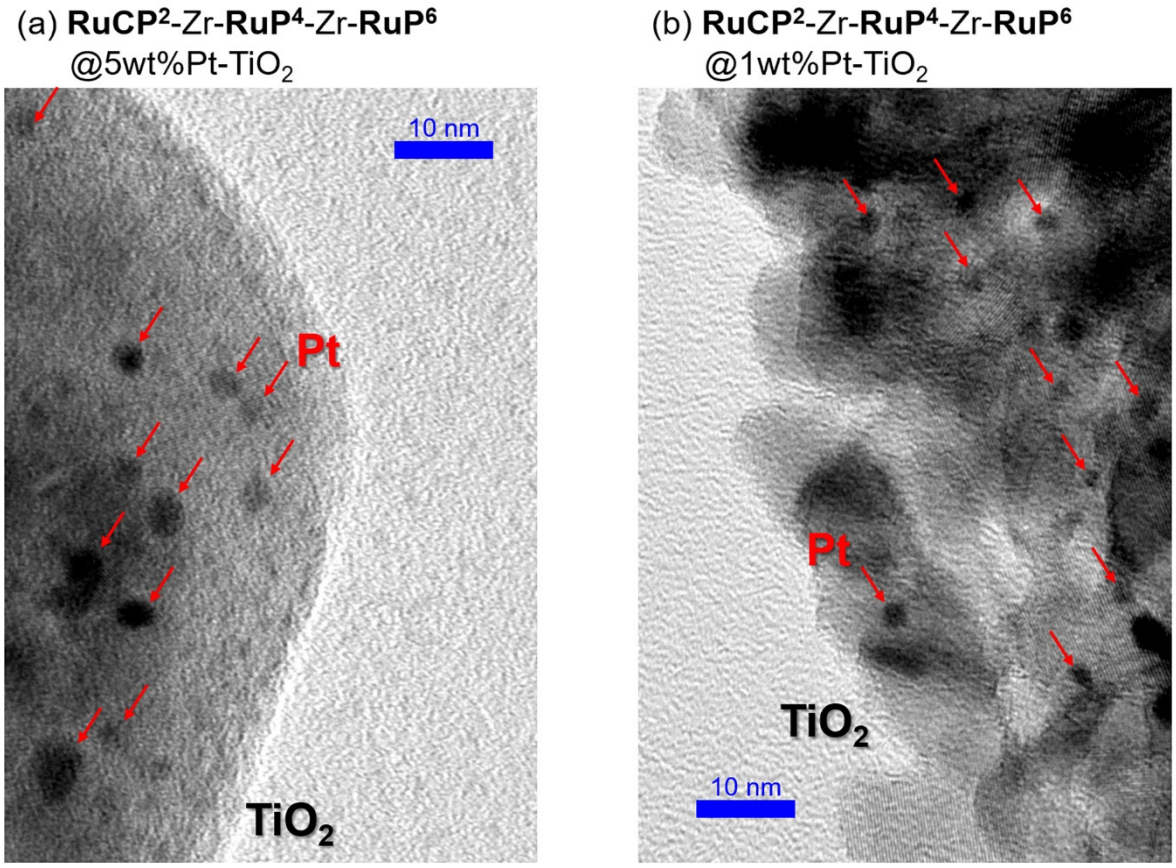

Figure S5. Transmission electron microscopic (TEM) images of (a) **RuCP^2**-Zr-**RuP^4**-Zr-**RuP^6**@5wt%Pt-TiO_2 and (b) **RuCP^2**-Zr-**RuP^4**-Zr-**RuP^6**@1wt%Pt-TiO_2. Red arrows indicate the Pt cocatalysts loaded on the surface of TiO_2.

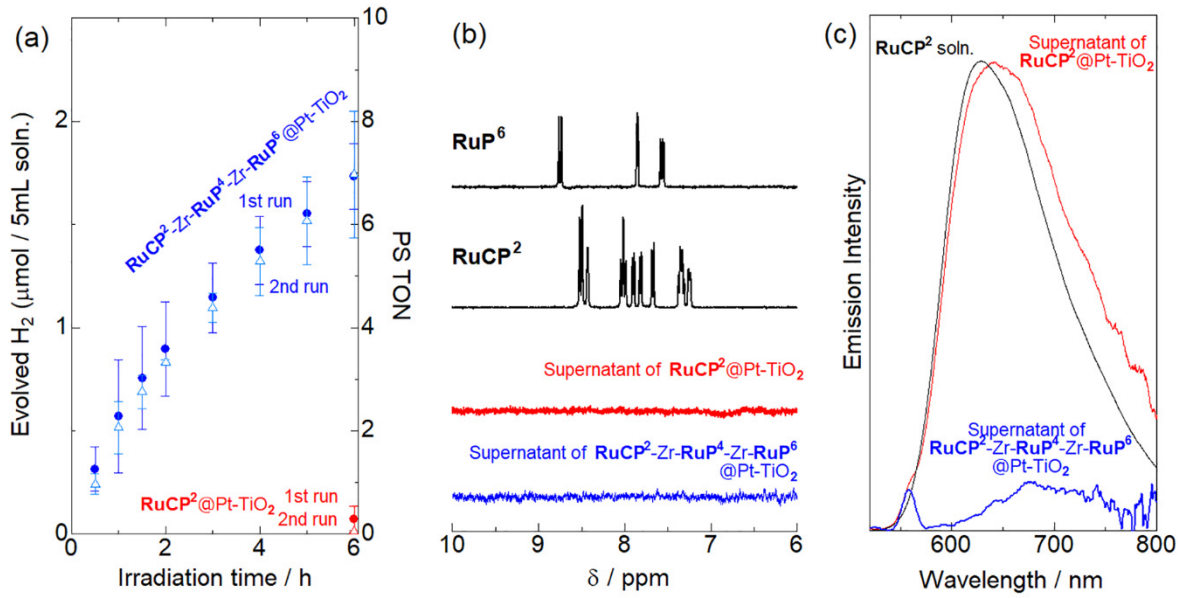

Figure S6. (a) Photocatalytic H_2 evolution reactions driven by **RuCP²**-Zr-**RuP⁴**-Zr-**RuP⁶**@Pt-TiO_2 (blue) or **RuCP²**@Pt-TiO_2 (red) in the presence of 0.5 M KI as the electron donor (100 μM Ru(II) dye, initial pH = 2.0, λ = 470 ± 10 nm). Closed circles and open triangles show the results of 1st and 2nd runs of the same nanoparticles. After the 1st run, the reaction solution was replaced by freshly prepared 0.5 M KI aqueous solution. (b) ^{1}H NMR (aromatic region) and (c) emission spectra of the supernatant solutions obtained after the 1st reaction of **RuCP²**-Zr-**RuP⁴**-Zr-**RuP⁶**@Pt-TiO_2 or **RuCP²**@Pt-TiO_2 by ultracentrifugation. Black lines in (b) are the spectra of **RuCP²** and **RuP⁶** in D_2O solvent. Black line in (c) shows the emission spectrum of **RuCP²** solution.

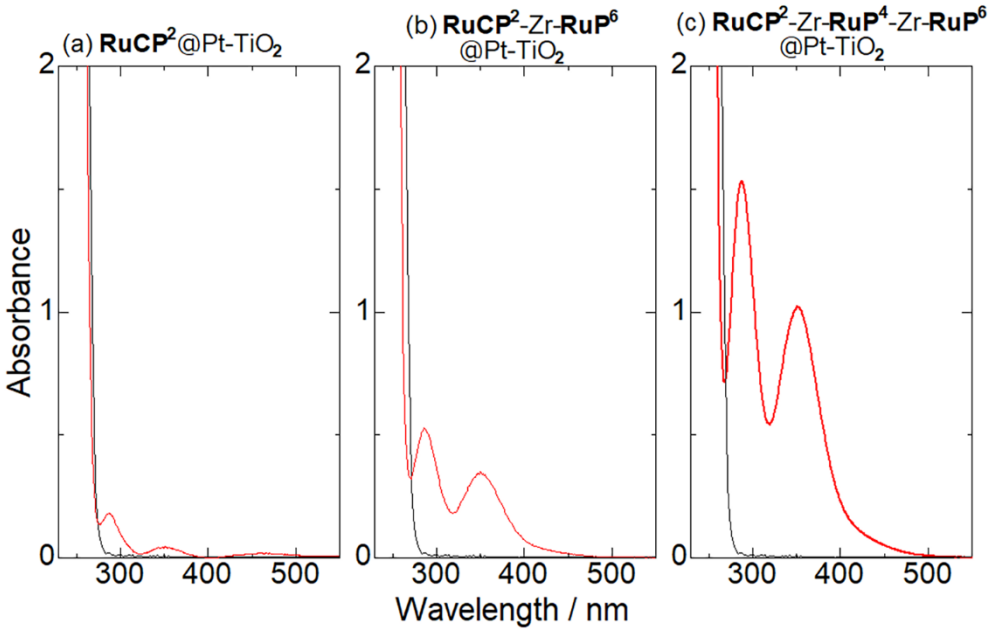

Figure S7. UV-Vis absorption spectral changes of the reaction solutions containing (a) **RuCP^2**@Pt-TiO_2, (b) **RuCP^2**-Zr-**RuP^6**@Pt-TiO_2, or (c) **RuCP^2**-Zr-**RuP^4**-Zr-**RuP^6**@Pt-TiO_2 nanoparticles and 0.5 M KI (black) before and (red) after photocatalytic H_2 evolution reaction for 6 h. The Ru(II)-PS-multilayered Pt-TiO_2 nanoparticles were removed by ultracentrifugation and each supernatant solution (1 mL) was diluted to 10 mL by the addition of water before the spectral measurement.

Table S3. Control experiments of photocatalytic hydrogen evolution of **RuCP^2**-Zr-**RuP^6**@Pt-TiO_2.

Entry [a]	Photocatalyst	Electron Donor (ED)	ED concentration	Light irradiation	Evolved H_2 [b]
1	**RuCP^2**-Zr-**RuP^6**@Pt-TiO_2	KI	0.5 M	Yes	Yes
2	**RuCP^2**-Zr-**RuP^6**@Pt-TiO_2	KBr	0.5 M	Yes	-
3	**RuCP^2**-Zr-**RuP^6**@Pt-TiO_2	NaI	0.5 M	Yes	Yes
4	**RuCP^2**-Zr-**RuP^6**@Pt-TiO_2	CsI	0.5 M	Yes	Yes
5	**RuCP^2**-Zr-**RuP^6**@Pt-TiO_2	$[Cu(dmp)_2]I$	Saturated	Yes	Yes
6	**RuCP^2**-Zr-**RuP^6**@Pt-TiO_2	$[Cu(dmp)_2]Cl$	Saturated	Yes	-
7	**RuCP^2**-Zr-**RuP^6**@Pt-TiO_2	-	-	Yes	-
8[c]	**RuCP^2**-Zr-**RuP^6**@Pt-TiO_2	$[Cu(dmp)_2]I$	Saturated	-	-
9[d]	-	$[Cu(dmp)_2]I$	Saturated	Yes	-
10	**RuCP^2**-Zr-**RuP^6**@Pt-TiO_2	$[Co(bpy)_3]Cl_2$	3 mM	Yes	-

[a] Reaction conditions: [Ru] = 100 μM in 20 mM CH_3COOH / CH_3COONa buffer aqueous solution (pH = 5, 5 mL) under blue LED light irradiation (λ = 470 ± 10 nm) for 6 h. [b] Gas in the head space was analyzed qualitatively by Gas Chromatography (GC). "Yes" indicates that the evolved amount of H_2 was larger than the GC detection limit.

Table S4. Zeta-potentials of Ru(II)-PS-immobilized nanoparticles in the absence/presence of 0.5 M KI aqueous solution (pH = 2.0).

Photocatalyst	without KI (mV)	with 0.5 M KI (mV)	with 0.5 M KBr (mV)
RuCP^2@Pt-TiO_2	−0.36	+3.6	-
RuCP^2-Zr-**RuP^6**@Pt-TiO_2	+45	−1.9	+4.00
RuCP^2-Zr-**RuP^4**-Zr-**RuP^6**@Pt-TiO_2	+38	−75	+7.46

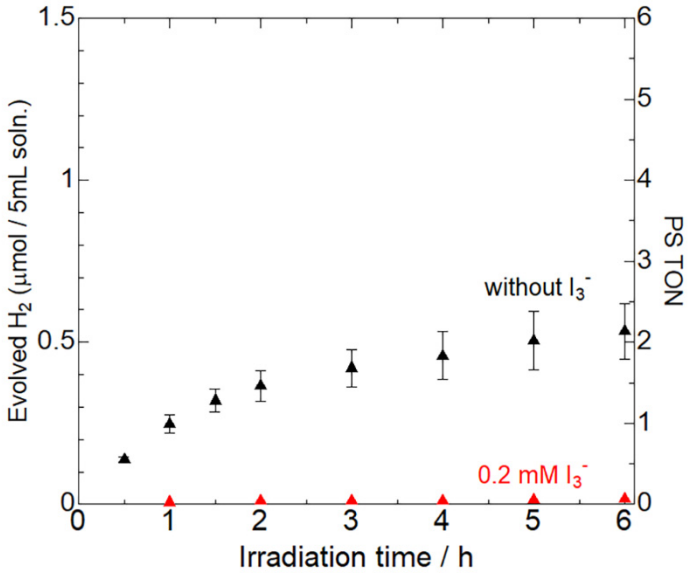

Figure S8. Triiodide ion-concentration-dependence of the photocatalytic H_2 evolution reaction of **RuCP²**-Zr-**RuP⁶**@Pt-TiO_2 nanoparticles (100 μM of the Ru(II) complex) in 0.5 M KI aqueous solution. Black and red triangles show the results in the absence and presence of 0.2 mM I_3^-, respectively. A blue LED light (λ = 470 ± 10 nm) was used as the irradiation source. The initial pH was adjusted to be 2.0 by adding HCl aq.

Table S5. Molar absorptivity and the absorbance of Ru(II)-PS-multilayered Pt-TiO_2 and triiodide at 470 nm after 6 h reaction solution.

	Molar absorptivity ($L \cdot cm^{-1} \cdot mol^{-1}$)		Absorbance after 6 h reaction	
Photocatalyst	I_3^-	Ru(II) dye	I_3^-	Ru(II) dye
RuCP²@Pt-TiO_2	754	14600	<0.01	1.46
RuCP²-Zr-**RuP⁶**@Pt-TiO_2	754	16249	0.08	1.62
RuCP²-Zr-**RuP⁴**-Zr-**RuP⁶**@Pt-TiO_2	754	16610	0.26	1.66

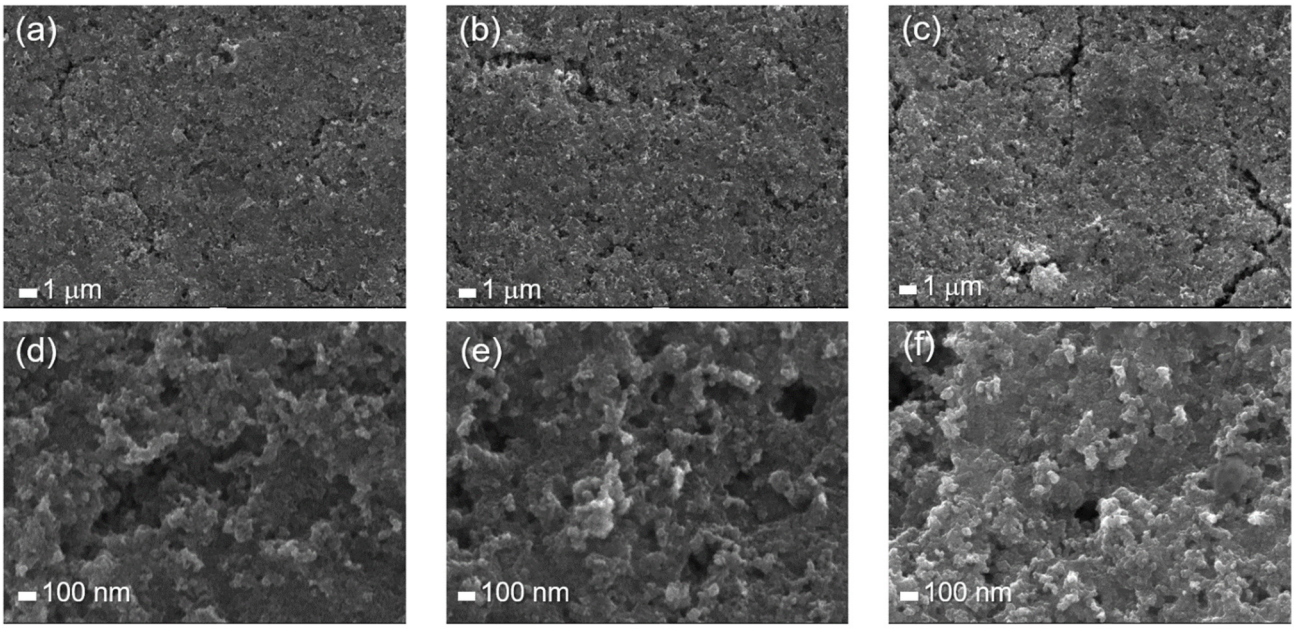

Figure S9. SEM images of (a, d) **RuCP^2**@TiO_2-ITO, (b, e) **RuCP^2**-Zr-**RuP^6**@TiO_2-ITO, (c, f) **RuCP^2**-Zr-**RuP^4**-Zr-**RuP^6**@TiO_2-ITO. The scale bar of (a-c) and (d-f) is 1 μm and 100 nm, respectively.

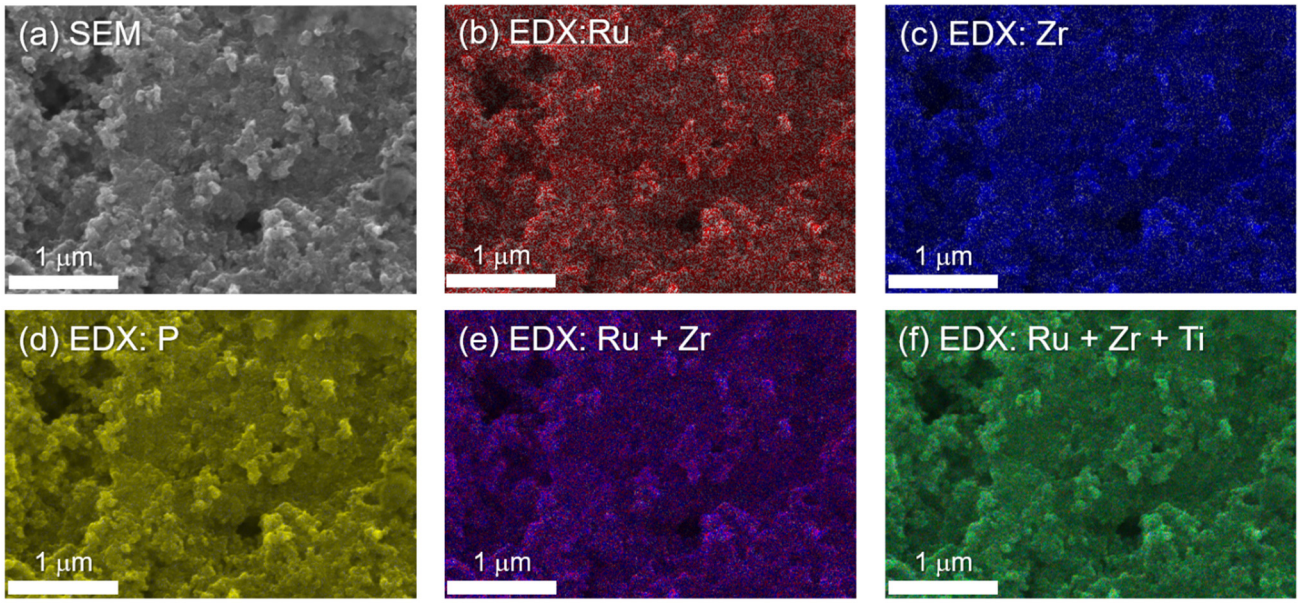

Figure S10. (a) SEM and (b-f) EDX images of **RuCP^2**-Zr-**RuP^4**-Zr-**RuP^6**@TiO_2-ITO of the elements (b) Ru, (c) Zr, (d) P, (e) Ru and Zr, (f) Ru , Zr, and Ti. Each scale bar is 1 μm.

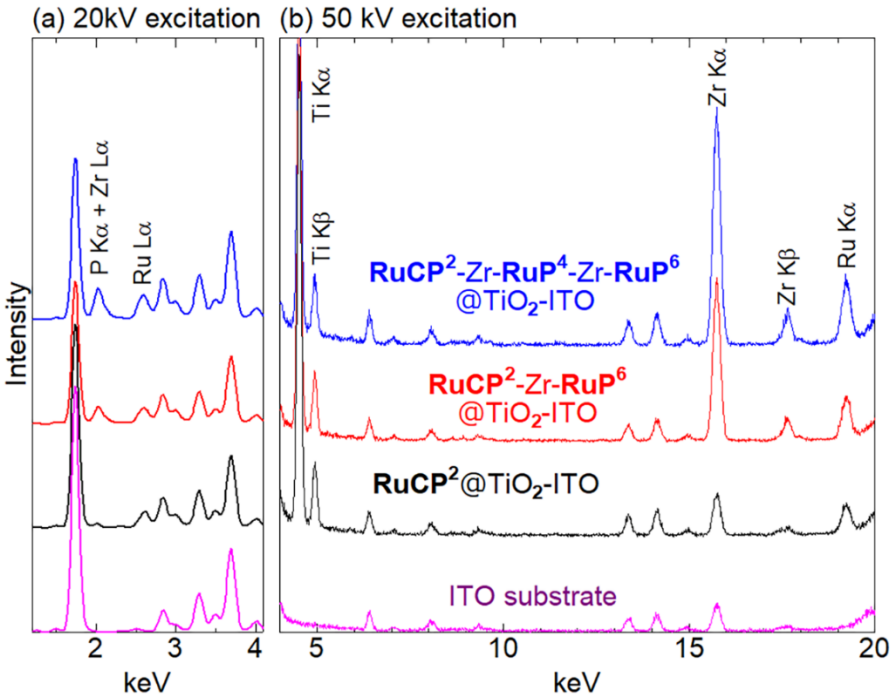

Figure S11. XRF spectra of ITO substrate (pink), **RuCP²**@TiO_2-ITO (black), **RuCP²**-Zr-**RuP⁶**@TiO_2-ITO (red), **RuCP²**-Zr-**RuP⁴**-Zr-**RuP⁶**@TiO_2-ITO (blue) in the solid state with (a) 20 kV and (b) 50 kV excitation. All spectra of Ru(II)-PS-multilayered TiO_2-ITO electrodes were normalized by using Ti Kβ peak.

Table S6. Immobilized amount of Ru(II) photosensitizer on TiO_2-ITO photoelectrode.

	Weight percentage of elements			
Photoelectrode	P	Ti	Zr	Ru
RuCP²-@TiO_2-ITO	1.75	97.99	-[a]	0.26
RuCP²-Zr-**RuP⁶**@TiO_2-ITO	7.16	91.26	1.26	0.32
RuCP²-Zr-**RuP⁴**-Zr-**RuP⁶**@TiO_2-ITO	12.87	85.13	1.58	0.42

[a] *Comparable intensity to that of bare ITO electrode was observed.*

Table S7. The photovoltaic data of DSSCs based on Ru(II)-PS-multilayered TiO_2-ITO photoanodes in methoxyacetonitrile (MAN) and water I^-/I_3^- electrolyte solutions.

	J_{SC} (mA / cm^2)		V_{OC} (V)		FF		PCE (%)	
Photoelectrode [c]	MAN[a]	Water[b]	MAN[a]	Water[b]	MAN[a]	Water[b]	MAN[a]	Water[b]
RuCP^2@TiO_2-ITO	0.063	-	0.148	-	0.24	-	0.002	-
RuCP^2-Zr-**RuP^6**@TiO_2-ITO	0.475	0.011	0.552	0.070	0.52	0.28	0.136	2.7 $\times10^{-4}$
RuCP^2-Zr-**RuP^4**-Zr-**RuP^6** @TiO_2-ITO	0.230	0.042	0.547	0.151	0.59	0.34	0.075	2.7 $\times10^{-3}$

[a] LiI (0.1 M), I_2 (0.05 M), and 0.5 M *t*-butyl-pyridine in methoxy-acetonitrile under AM1.5G irradiation. [b] KI (0.5 M), and I_2 (0.05 M), in water (pH = 2) under blue light irradiation (λ_{ex} = 470 nm, 800 W/m^2). [c] A PEDOT-TMA coated ITO electrode was used as the counter electrode.

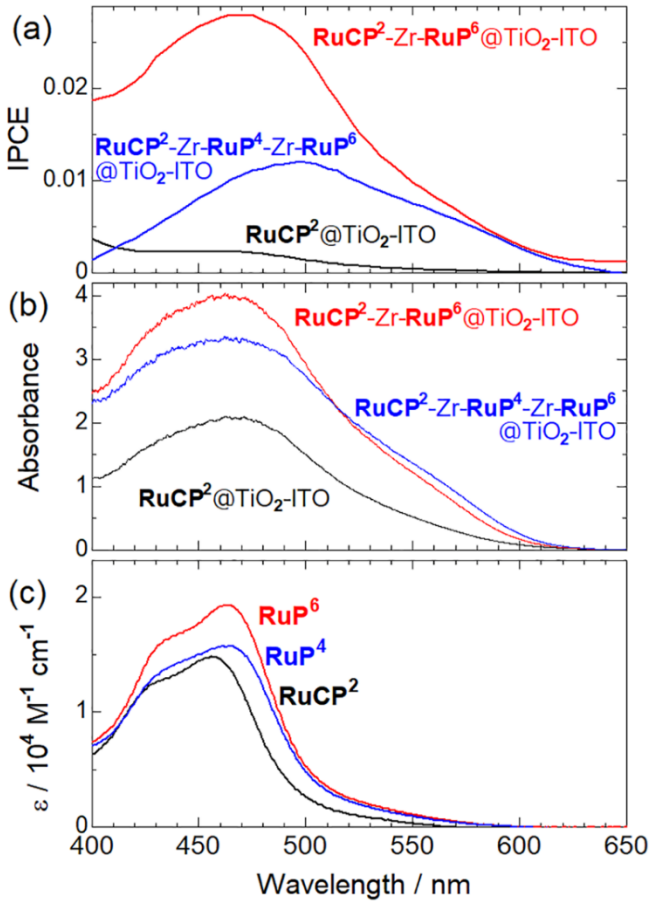

Figure S12. (a) IPCE action spectra of (black) **RuCP^2**@TiO_2-ITO, (red) **RuCP^2**-Zr-**RuP^6**@TiO_2-ITO, or (blue) **RuCP^2**-Zr-**RuP^4**-Zr-**RuP^6**@TiO_2-ITO as the photoanode in the presence of LiI (0.1 M), I_2 (0.05 M), and 0.5 M *t*-butyl-pyridine in methoxy-acetonitrile under AM1.5G irradiation. A PEDOT-TMA coated ITO electrode was used as the counter electrode. (b) UV-Vis diffuse reflectance spectra of these photoelectrodes in air. (c) UV-Vis absorption spectra of (red) **RuP^6**, (blue) **RuP^4**, and (black) **RuCP^2** dyes in water (pH = 2.2).

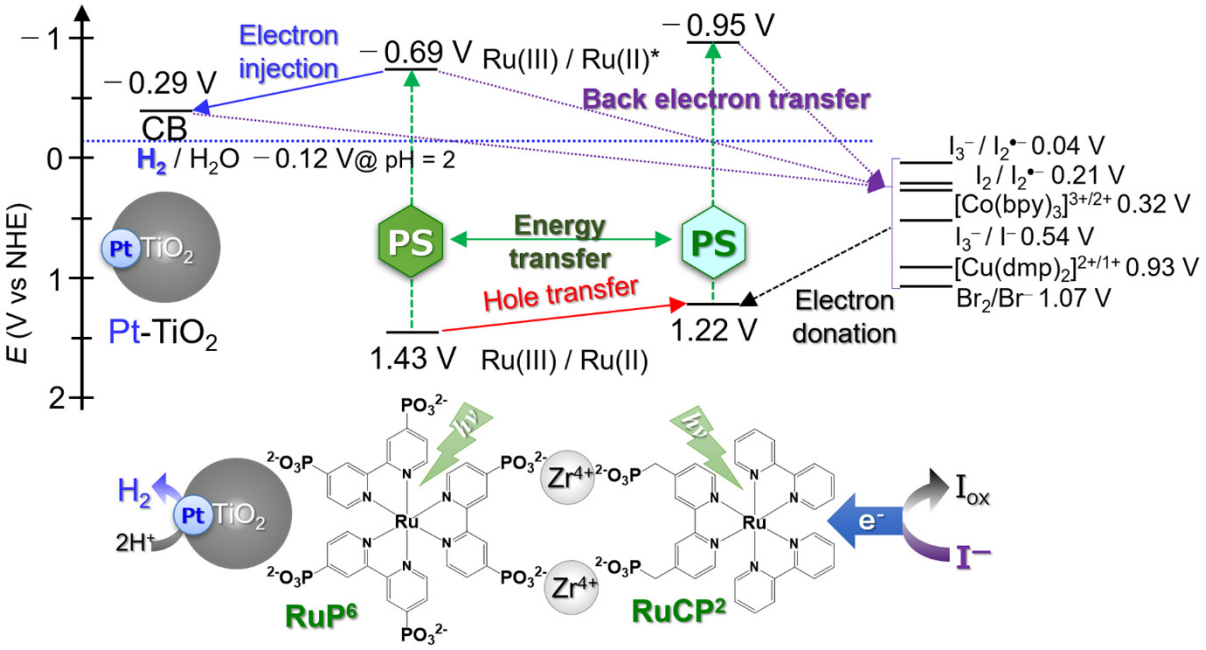

Scheme S1. Schematic diagram showing a plausible energy and electron transfer mechanism of **RuCP²**-Zr-**RuP⁶**@Pt-TiO_2. Redox potentials of bromide, iodide species, $[Co(bpy)_3]^{3+/2+}$ and $[Cu(dmp)_2]^{2+/1+}$ complexes are interfered from the literatures.[2,3,4]

References.

1. Y. Kijitori, M. Ikegami, T. Miyasaka, *Chem. Lett.*, 2007, **36**, 190-191.
2. L. Troian-Gautier, M. D. Turlington, S. A. M. Wehlin, A. B. Maurer, M. D. Brady, W. B. Swords, G. J. Meyer, Halide Photoredox Chemistry, *Chem. Rev.* 2019, **119**, 4628-4683.
3. Y. Sasaki, H. Kato, A. Kudo, *J. Am. Chem. Soc.* 2013, **135**, 5441-5449.
4. Y. Saygili, M. Söderberg, N. Pellet, F. Giordano, Y. Cao, A. B. Muñoz-García, S. M. Zakeeruddin, N. Vlachopoulos, M. Pavone, G. Boschloo, L. Kavan, J.-E. Moser, M. Grätzel, A. Hagfeldt, M. Freitag, *J. Am. Chem. Soc.* 2016, **138**, 15087-15096.